The average first shell coordination distance increased by an average of 0.12 Å from the diferric to the diferrous state. The data and fits for the two diferrous protein samples are essentially identical, although **EXAFS3** had higher coordination numbers than **EXAFS6**. For deoxyhemerythrin, the average first shell coordination was 2.15 Å by EXAFS analysis, and the average first shell coordination of the diferrous hydroxylase, 2.15 Å, is in good agreement with that number. The peak associated with the metal-metal interaction is missing for both reduced hydroxylase protein samples, suggesting that the absence of a Fe···Fe backscattering peak is inherent in the structure of the samples, and not an artifact of the data collection or analysis. A 3.57 Å Fe···Fe distance has been reported for deoxyhemerythrin.[48]

Conclusions. While initial EPR studies suggested that the active site of the MMO hydroxylase is similar to the dinuclear iron centers found in Hr and RRB2, our results indicate some striking differences. The hydroxylase does not contain an oxo-bridged diiron core like that observed in Hr and RRB2. The 3.4 Å Fe···Fe distance, the intermediate Mössbauer quadrupole splitting, the semimet J value of -32 cm^{-1}, and the featureless absorption spectrum indicate that the hydroxylase contains a novel Fe···Fe bridge. We believe that the diiron center may contain an alkoxo, a hydroxo, or a monodentate carboxylato bridge, and one or two bidentate bridging carboxylates. The coordination of the Fe atoms has yet to be conclusively determined. We have also reported a model dependence for EXAFS results, which has important implications for the determination of Fe···Fe distances by EXAFS.

Acknowledgment. The data were collected at the Stanford Synchrotron Radiation Laboratory and the National Synchrotron Light Source, Brookhaven National Laboratory, which are supported by the Department of Energy, Office of Basic Energy Sciences, Division of Chemical Sciences and Division of Materials Sciences. SSRL is also supported by the National Institutes of Health, Biomedical Resource Technology Program, Division of Research Resources (RR-01209). Grant support was provided by the National Science Foundation (CHE 88-17702 to K.O.H.), the Gas Research Institute (5086-260-1209 to H.D.), and the National Institute of General Medical Sciences (GM 32134 to S.J.L.). J.G.B. acknowledges support as an American Cancer Society Postdoctoral Fellow. $[Fe_2O(O_2CH)_4(BIPhMe)_2]$ was kindly provided by Dr. William B. Tolman.

Registry No. Fe, 7439-89-6; $[Fe_2O(O_2CH)_4(BIPhMe)_2]$, 123594-49-0; hydroxylase, 9046-59-7; methane monooxygenase, 51961-97-8.

Supplementary Material Available: Table S1 giving results of wide shell fits to the hydroxylase (2 pages). Ordering information is given on any current masthead page.

Control of Magnetic Interactions in Polyarylmethyl Triplet Diradicals Using Steric Hindrance

Andrzej Rajca,*,† Suchada Utamapanya, and Jiangtien Xu

Contribution from the Department of Chemistry, Kansas State University, Manhattan, Kansas 66506. *Received May 17, 1991. Revised Manuscript Received July 26, 1991*

Abstract: Three polyarylmethyl triplet diradicals are prepared by oxidation of the corresponding carbodianions. Solid-state studies of the diradicals using SQUID show an onset of short-range ferromagnetic interactions at temperatures below 4 K for diradical $3^{2\bullet}$ and antiferromagnetic interactions below 70 K for diradicals $2^{2\bullet}$ and $4^{2\bullet}$. The diradicals and the corresponding carbodianions in solution are characterized using ESR, NMR, and UV-vis spectroscopy, and voltammetry.

Introduction

Organic magnets may offer a novel insight into the nature of magnetism and may lead to materials with combined unusual optical, electrical, and magnetic properties.[1] In most organic molecular solids composed of open-shell molecules, the unpaired electrons interact weakly and, if a significant interaction takes place, it is usually antiferromagnetic. Such solids are either bulk paramagnets or, if antiferromagnetic interactions lead to a long-range ordering of unpaired spins, antiferromagnets. Several exceptional organic solids have been found to possess weak ferromagnetic intermolecular interactions: dinitroxy,[2] nitronyl oxide,[3] galvinoxyl,[4] and nitrophenyl verdazyl.[5] However, none of these solids is a ferromagnet. Ferromagnetic interactions are prerequisite to most interesting magnetic properties.[6] Thus, the ability to design solids with ferromagnetic interactions in a rational manner is important and intellectually challenging.

In 1963, McConnell used a simple theory to propose that a nearest-neighbor π-overlap of the sites with the opposite sign spin densities located at adjacent molecules should lead to intermolecular ferromagnetic coupling.[7] Many π-conjugated radicals and polyradicals possess such alternating sign spin densities.[8] Izuoka, Murata, Sugawara, and Iwamura showed that the coupling between two triplet carbenes in a cyclophane framework can be predicted using the McConnell model.[9] Similarly, the ferromagnetic vs antiferromagnetic coupling was correlated with X-ray structures for two solid monoradicals.[5]

Now we report the preparation, spectroscopy, and solid-state studies on triplet diradicals $2^{2\bullet}$, $3^{2\bullet}$, and $4^{2\bullet}$ (Figure 1). $2^{2\bullet}$, $3^{2\bullet}$, and $4^{2\bullet}$ are derivatives of previously reported diradicals $1^{2\bullet}$, Schlenk hydrocarbon $5^{2\bullet}$, and perchlorinated Schlenk hydrocarbon.[10-12]

† The Camille and Henry Dreyfus Teacher-Scholar, 1991.

(1) Carter, F. L., Ed. *Molecular Electronic Devices*; Marcel Dekker: New York, 1982 and 1987; Vols. I and II.
(2) Saint Paul, M.; Veyret, C. *Phys. Lett. A* **1973**, *45*, 362. Chouteau, G.; Veyret-Jeandey, C. *J. Phys.* **1981**, *42*, 1441.
(3) Awaga, K.; Maruyama, Y. *Chem. Phys. Lett.* **1989**, *158*, 556. Awaga, K.; Maruyama, Y. *J. Chem. Phys.* **1989**, *91*, 2743. Awaga, K.; Inabe, T.; Nagashima, U.; Maruyama, Y. *J. Chem. Soc., Chem. Commun.* **1989**, 1617; **1990**, 520.
(4) Awaga, K.; Sugano, T.; Kinoshita, M. *J. Chem. Phys.* **1986**, *85*, 2211. Kinoshita, M. *Mol. Cryst. Liq. Cryst.* **1990**, *176*, 163.
(5) Allemand, P.-M.; Srdanov, G.; Wudl, F. *J. Am. Chem. Soc.* **1990**, *112*, 9391. The correlation is between room temperature structure and magnetic interactions in the liquid helium temperature range.
(6) Carlin, R. L. *Magnetochemistry*; Springer-Verlag: Berlin, 1986.
(7) McConnell, H. M. *J. Chem. Phys.* **1963**, *39*, 1910.
(8) Mataga, N. *Theor. Chim. Acta* **1968**, *10*, 372. Ovchinnikov, A. A. *Theor. Chim. Acta* **1978**, *47*, 497. Wertz, J. E.; Bolton, J. R. *Electron Spin Resonance*; Chapman: New York, 1986; Chapter 6.
(9) Izuoka, A.; Murata, S.; Sugawara, T.; Iwamura, H. *J. Am. Chem. Soc.* **1987**, *109*, 2631.
(10) Rajca, A. *J. Am. Chem. Soc.* **1990**, *112*, 5890.

0002-7863/91/1513-9235$02.50/0

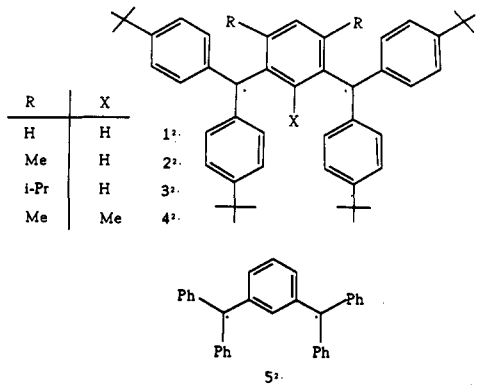

Figure 1.

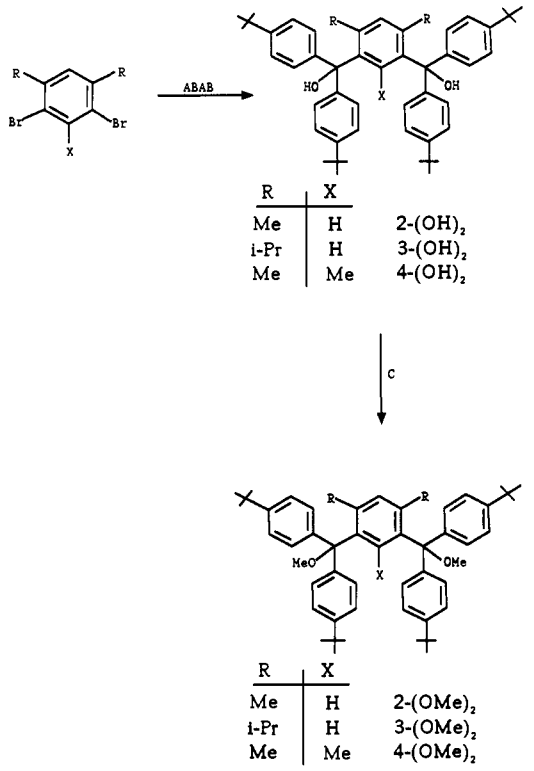

Figure 2. Synthesis of the ether precursors: A = *t*-BuLi, ether; B = 4,4'-di-*tert*-butylbenzophenone; C = MeOH, $(CF_3CO)_2O$, CH_2Cl_2.

Alkyl substituents ("R" and "X") increase the stability of $2^{2\bullet}$, $3^{2\bullet}$, and $4^{2\bullet}$ to the extent that they can be studied in the solid state. Use of triplet diradicals instead of monoradicals may be helpful in achieving large magnetic interactions.

We would like to explore the possibility that steric hindrance may be used to control the orientation of diradicals in the solid state and, therefore, induce either antiferromagnetic or ferromagnetic intermolecular interactions. Our working hypothesis is that for large alkyl groups R (Figure 1), the steric repulsion between the R groups (or the neighboring benzene rings twisted out-of-plane by R) in adjacent molecules should cause an antiparallel stacking; conversely, for small R, the diradicals may stack in a "parallel" orientation to each other. In the first case, the intermolecular overlap is most likely between sites of opposite sign spin densities (both large positive or both small negative) and, according to the McConnell model, the ferromagnetic coupling should be observed; in the second case, the antiferromagnetic coupling should result. Therefore, solid diradical $3^{2\bullet}$ should possess

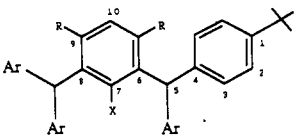

Figure 3.

Table I. Selected NMR (THF-d_8) and ESR (2-MeTHF) Spectral Data: ^{13}C Chemical Shifts for C-1 for Dianions and Zero-Field Parameters ($|D/hc|$) for Diradicals

	1	2	3	4
δ (ppm)	133.5[a]	128.5	127.4	125.9
$\lvert D/hc\rvert$ (10^{-3}, cm^{-1})[c]	6.6[b]	8.7	9.9	10.7

[a] Reference 14. [b] $|D/hc| = 6.4 \times 10^{-3}$ cm^{-1} in THF (ref 10). [c] $|D/hc| = 7.9 \times 10^{-3}$ cm^{-1} for $5^{2\bullet}$ (ref 11).

Table II. UV–Vis Spectral Data for Dianions (THF) and Diradicals (THF/Toluene)

	λ_{max} (nm)	
	dianion	diradical
1	480[a]	
2	463	352
3	463	352[b]
4	471	349

[a] The following paper in this issue. [b] 350 nm in THF.

intermolecular ferromagnetic interactions, and solid diradicals $2^{2\bullet}$ and $4^{2\bullet}$ should possess intermolecular antiferromagnetic interactions.

Results and Discussion

Synthesis of Precursors. Consecutive lithiations of dibromobenzenes with *t*-BuLi and quenching of the organolithium compounds with 4,4'-di-*tert*-butylbenzophenone gave diols **2**-$(OH)_2$, **3**-$(OH)_2$, and **4**-$(OH)_2$ (Figure 2). Treatment of diols **2**-$(OH)_2$, **3**-$(OH)_2$, and **4**-$(OH)_2$ with MeOH/trifluoroacetic anhydride produces the corresponding diethers **2**-$(OMe)_2$, **3**-$(OMe)_2$, and **4**-$(OMe)_2$. The diols are also converted to dihalides **2**-$(Hal)_2$ and **3**-$(Hal)_2$ (hydroxyl groups in diols are replaced with Cl or Br) using HCl gas, HBr gas, or $SOCl_2$/hexane.[13]

Carbodianions. Treatment of ether precursors **2**-$(OMe)_2$, **3**-$(OMe)_2$, and **4**-$(OMe)_2$ with lithium metal in tetrahydrofuran (THF) produces the corresponding carbodianions 2^{2-},$2Li^+$, 3^{2-},$2Li^+$, and 4^{2-},$2Li^+$ (Scheme I).[14] Solutions of carbodianions are separated from precipitated MeOLi by decantation. When the solutions of the dianions are quenched with MeOH, hydrocarbons **2**-$(H)_2$, **3**-$(H)_2$, and **4**-$(H)_2$ are isolated in high chemical yields (Scheme I).

Solutions of carbodianions in THF-d_8 are examined by ^1H and ^{13}C NMR spectroscopy. No MeOLi can be detected (<5%). The spectra are comparable to those reported for the related carbodianion 1^{2-},$2Li^+$ except for line-broadening in the aromatic region of the ^1H NMR spectra at 303 K.[14] Variable-temperature ^1H and ^{13}C NMR spectra of 2^{2-},$2Li^+$ suggest that the rotation of the 4-*tert*-butylphenyl groups can be made slow on the NMR time scale; that is, at low temperature all 4-*tert*-butylphenyl groups are equivalent, but the exo and endo sides of each group become nonequivalent. The coalescence of the protons, which are tentatively assigned as ortho in the 4-*tert*-butylphenyl groups, is observed at about 260 K. Similar coalescence is detected for ortho and meta carbon nuclei at about 260 and 230 K, respectively.

^{13}C chemical shifts for para carbons in arylmethyl carbanions can be used to measure negative charge delocalization to the benzene ring.[15] In dianions 1^{2-},$2Li^+$, 2^{2-},$2Li^+$, 3^{2-},$2Li^+$, and 4^{2-},$2Li^+$ one such para carbon, C-1, is particularly useful because of its remoteness from alkyl R substituents (Figure 3). In fact,

(11) Kothe, G.; Denkel, K.-H.; Summermann, W. *Angew. Chem., Int. Ed. Engl.* **1970**, *9*, 906. Luckhurst, G. R.; Pedulli, G. F. *J. Chem. Soc. B* **1971**, 329.

(12) Veciana, J.; Rovira, C.; Crespo, M. I.; Armet, O.; Domingo, V. M.; Palacio, F. *J. Am. Chem. Soc.* **1991**, *113*, 2552.

(13) Dihalides are difficult to purify.

(14) Rajca, A. *J. Am. Chem. Soc.* **1990**, *112*, 5889.

(15) O'Brien, D. H. In *Comprehensive Carbanion Chemistry*; Buncle, E., Durst, T., Eds.; Elsevier: Amsterdam, 1980; Chapter 6.

Table III. Cyclic Voltammetric (CV) Data and Differential Pulse Voltammetric (DPV) Data[a] for Dianions and Diradicals in THF/TBAP

	CV (V ± 20 mV)				DPV (V ± 20 mV)		
	first oxidation		second oxidation				
	$E_{p,1}$	$\Delta E_{p,1}$	$E_{p,2}$	$\Delta E_{p,2}$	$E_{DP,1}$	$E_{DP,2}$	ΔE_{DP}
1^{2-}	−1.50[b]	0.08	−1.26	0.10	−1.54	−1.33	0.21
2^{2-}	−1.48	0.10	−1.33	0.11	−1.55	−1.39	0.16
3^{2-}	−1.48	0.12	−1.33	0.12	−1.58	−1.41	0.17
4^{2-}	−1.52	0.10	−1.31	0.11			
	CV (V ± 20 mV)				DPV (V ± 20 mV)		
	first reduction		second reduction				
	$E_{p,1}$	$\Delta E_{p,1}$	$E_{p,2}$	$\Delta E_{p,2}$	$E_{DP,1}$	$E_{DP,2}$	ΔE_{DP}
$2^{2\cdot}$	−1.43	0.12	−1.56	0.10			
$3^{2\cdot}$	−1.47	0.12	−1.60	0.09			
$4^{2\cdot}$	−1.45	0.10	−1.68	0.09	−1.36	−1.59	0.23

[a] Potentials vs Ag wire quasi-reference electrode. [b] The following paper in this issue.

Scheme I

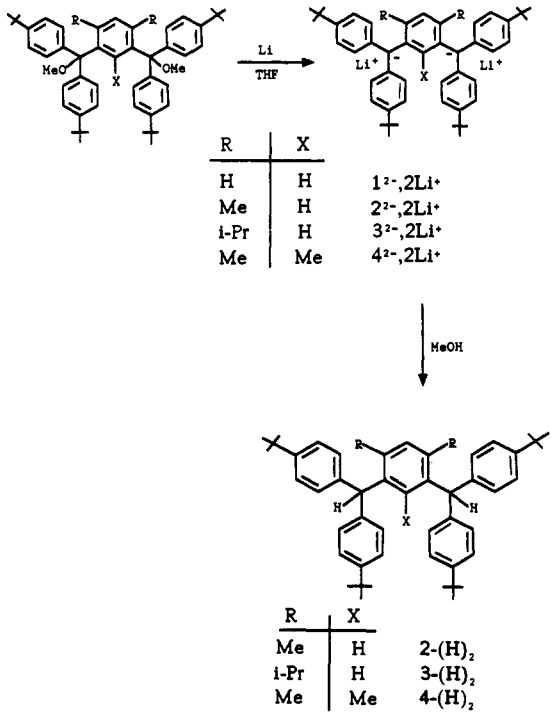

the ^{13}C chemical shift for C-1 moves progressively upfield in dianions 1^{2-},2Li$^+$, 2^{2-},2Li$^+$, 3^{2-},2Li$^+$, and 4^{2-},2Li$^+$, that is, there is an increase in negative charge delocalization to the 4-*tert*-butylphenyl groups (Table I).

UV–vis spectra for carbodianions 2^{2-},2Li$^+$, 3^{2-},2Li$^+$, and 4^{2-},2Li$^+$ in THF have broad bands with λ_{max} values that are similar to the parent carbodianion, 1^{2-},2Li$^+$ (Table II).

Carbodianions 1^{2-},2Li$^+$, 2^{2-},2Li$^+$, 3^{2-},2Li$^+$, and 4^{2-},2Li$^+$ have two reversible oxidation waves in cyclic voltammetry (CV) in the range from −1.6 to −1.3 V that correspond to the radical anion and the diradical (Figure 4, Table III). Thus, the oxidation potentials are similar for all carbodianions. The waves are separated by about 200 mV for each dianion, which is significantly more than the 35-mV difference expected for two one-electron transfers from two noninteracting groups.[16]

(16) When there is no interaction between the redox groups, i.e., when the statistical factors interfere, the potential separation between the CV waves for the first and kth electron transfer should be $(2RT/F)$ ln k. For two groups, i.e., in a dianion, $k = 2$ and the potential difference is 35.6 mV at 25 °C, see: Bard, A. J.; Faulkner, L. R. *Electrochemical Methods*; Wiley: New York, 1980; Chapter 6, p 234. From a potential difference of about 200 mV for two consecutive one-electron reductions of a diradical, a disproportionation equilibrium constant, $K_d = \exp[\Delta E_{1/2}F/RT]$, for a radical anion to dianion and diradical should be about 10^{-3} at ambient temperature (the radical anion should predominate); for example, see: Hill, M. G.; Mann, K. R. *Inorg. Chem.* **1991**, *30*, 1429.

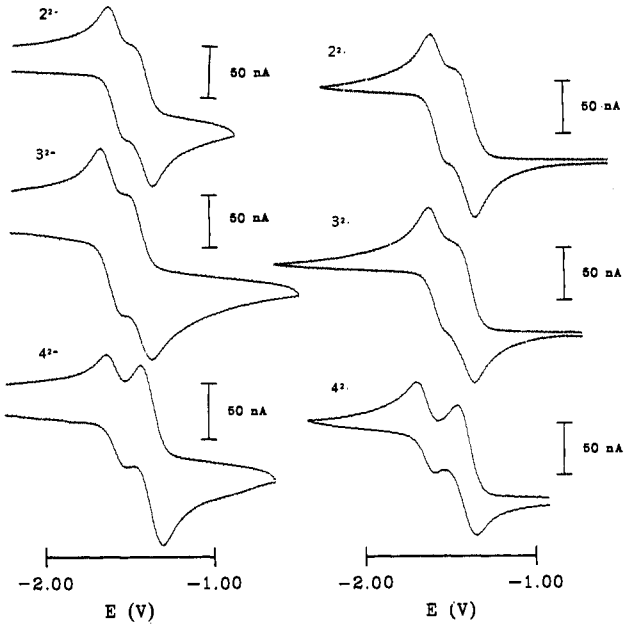

Figure 4. Cyclic voltammetry spectra for carbodianions 2^{2-}, 3^{2-}, and 4^{2-} and diradicals $2^{2\bullet}$, $3^{2\bullet}$, and $4^{2\bullet}$ in THF/TBAP. (Solid diradicals are dissolved in THF.)

Scheme II

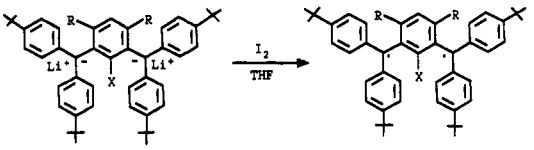

The oxidation waves corresponding to radical cations and dications are only partially reversible and are located in the positive potential range 0.3–0.5 V. The CV data are further corroborated by differential pulse voltammetry (DPV) measurements (Table III). In particular, for both 2^{2-} and 3^{2-}, the radical anion/diradical DPV peak oxidation currents are identical. (Oxidation currents are more difficult to infer from overlapped CV waves.)

Diradicals. Treatment of 0.04 M solutions of carbodianions 2^{2-},2Li$^+$, 3^{2-},2Li$^+$, and 4^{2-},2Li$^+$ in THF with 1 molar equiv of iodine at 273 K for 15 min produces solutions of the corresponding diradicals $2^{2\bullet}$, $3^{2\bullet}$, and $4^{2\bullet}$ (Scheme II).[10]

After a 10-fold dilution with 2-methyltetrahydrofuran (2-MeTHF) or toluene, the solutions are examined by ESR spectroscopy. The $\Delta m_s = 1$ regions of the ESR spectra at 100 K for diradicals $2^{2\bullet}$, $3^{2\bullet}$, and $4^{2\bullet}$ consist of four symmetrical peaks, which are assigned to the triplet state with the approximate zero-field degeneracy, $|E/hc| \approx 0$. The center peak in the spectrum corresponds to a doublet impurity and, typically, its peak height is comparable to the triplet peaks (Figure 5).[17] A half-field Δm_s

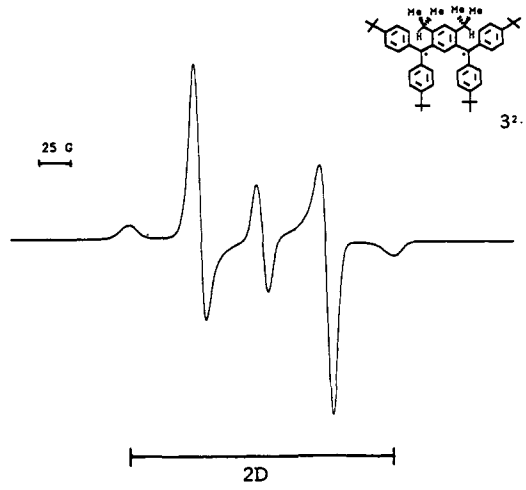

Figure 5. ESR spectrum for diradical $3^{2\bullet}$ in 2-MeTHF glass at 100 K. (Solid diradical $3^{2\bullet}$ is dissolved in 2-MeTHF.) Typically, for spectra of *crude* diradicals $2^{2\bullet}$, $3^{2\bullet}$, and $4^{2\bullet}$ in THF/2-MeTHF or THF/toluene, the height for the center peak (doublet impurities) is less than the height for triplet resonances.

= 2 resonance is also observed for each diradical. The spectra are practically identical in either 2-MeTHF or toluene glass. The other zero-field parameter, $|D/hc|$, for diradicals $2^{2\bullet}$, $3^{2\bullet}$, and $4^{2\bullet}$ increases in that order and is significantly greater compared to the parent diradical $1^{2\bullet}$ (Table I, Figure 5). Because $|D/hc|$ for a triplet is related to the strength of the magnetic dipole–dipole interaction between "unpaired electrons", larger values of $|D/hc|$ might suggest smaller average distances between the "unpaired electrons" in diradicals.

Because the diradicals and the dianions differ in the population of the two nonbonding MO's only, charge distribution in dianions may be similar to spin distribution in diradicals.[14] According to the preceding NMR data, negative charge in the *4-tert*-butylphenyl groups in the dianions increases in the same order as the $|D/hc|$ values for diradicals. For approximately planar π-conjugated systems, this NMR and ESR data would imply a different response of the negative charge and spin to steric hindrance in dianions and diradicals, respectively. Nonplanarity for the π-conjugated systems **2**, **3**, and **4** complicates the interpretation of the data, e.g., through-space interactions may affect $|D/hc|$. Furthermore, in dianions, steric hindrance may change the charge distribution (^{13}C chemical shifts) by perturbation of ion pairing.

After examination using ESR spectroscopy, solutions of diradicals $2^{2\bullet}$, $3^{2\bullet}$, and $4^{2\bullet}$ in toluene/THF are further diluted with toluene, and the UV–vis spectra at ambient temperature are obtained. Diradicals $2^{2\bullet}$, $3^{2\bullet}$, and $4^{2\bullet}$ have $\lambda_{max} = 350 \pm 2$ nm (Table II, Figure 6). The $\lambda_{max} = 348$ nm is also observed for the related doublet monoradical, tris(4-*tert*-butylphenyl)methyl.[18]

Following the ESR spectroscopic examination, the solutions of diradicals $2^{2\bullet}$, $3^{2\bullet}$, and $4^{2\bullet}$ in 2-MeTHF/THF are reduced with lithium metal to carbodianions and, subsequently, quenched with MeOH. The resultant hydrocarbons **2**-$(H)_2$, **3**-$(H)_2$, and **4**-$(H)_2$ possess identical spectral data compared to the quenching products prepared using carbodianions that are directly generated from the diether precursors.

In order to further ascertain the structure of the diradicals, a traditional route to polyarylmethyl radicals using dihalides is employed. When dihalides **2**-$(Hal)_2$ and **3**-$(Hal)_2$ are subjected to halogen abstraction using zinc powder in toluene, the ESR spectra of diradicals $2^{2\bullet}$ and $3^{2\bullet}$ are comparable to those obtained via iodine oxidation of carbodianions; however, the amount of a doublet impurity is significant.[13]

Solid-State Studies. Solutions (0.1 M) of diradicals $2^{2\bullet}$, $3^{2\bullet}$, and $4^{2\bullet}$ in THF are prepared at 273 K using the carbanion method.

(17) Only a fraction of the triplet diradical contributes to its signal intensity in a randomly oriented glass sample.

(18) ESR of tris(4-*tert*-butylphenyl)methyl: Van der Hart, W. J. *Mol. Phys.* **1970**, *19*, 75.

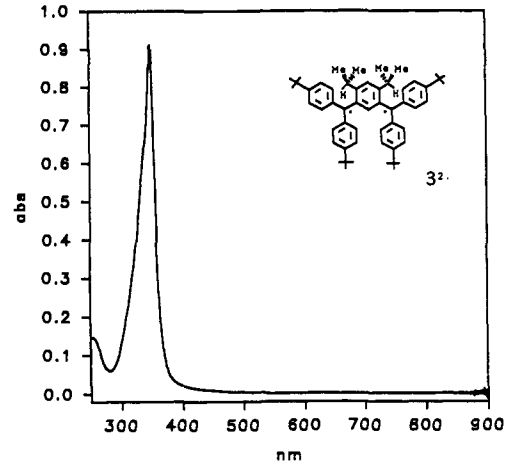

Figure 6. UV–vis spectrum for diradical $3^{2\bullet}$ in THF. (Solid diradical $3^{2\bullet}$ is dissolved in THF.) The spectra for diradicals $2^{2\bullet}$, $3^{2\bullet}$, and $4^{2\bullet}$ in THF/toluene possess similar band shapes and $\lambda_{max} = 350 \pm 2$ nm (Table II).

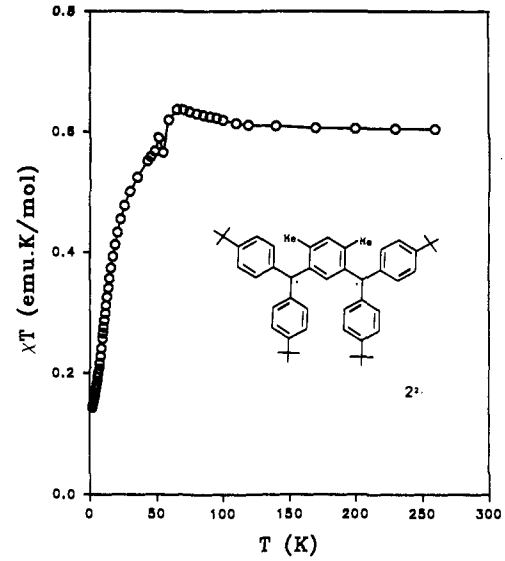

Figure 7. Plot of the product of magnetic susceptibility and temperature vs temperature for $2^{2\bullet}$. SQUID data obtained at $H = 500$ Oe.

THF is removed on a vacuum line. The solid residues are repeatedly treated with degassed MeOH to wash out LiI (a side product of the oxidation) and then dried under high vacuum. The solid diradicals can be stored under argon at ambient temperature in a glovebox and do not change significantly over several days.

Solutions, which are prepared by dissolving the solids $2^{2\bullet}$, $3^{2\bullet}$, and $4^{2\bullet}$ in an appropriate solvent, are examined by ESR spectroscopy (2-MeTHF), UV–vis spectroscopy (THF), and electrochemistry (THF/TBAP). For example, ESR and UV–vis spectra for diradical $3^{2\bullet}$ are shown in Figures 5 and 6.

In the ESR spectrum of $3^{2\bullet}$, the amount of doublet impurities is significantly reduced compared to the preceding spectra of the crude reaction mixtures. However, the ESR spectra of solid $2^{2\bullet}$ and $4^{2\bullet}$ dissolved in 2-MeTHF show more doublet impurities compared to the preceding spectra of the crude reaction mixtures.

The shown UV–vis spectrum is similar to the spectra of crude reaction mixtures in toluene/THF and is typical of all three diradicals, $2^{2\bullet}$, $3^{2\bullet}$, and $4^{2\bullet}$ (Figure 6, Table II). Cyclic voltammetry and differential pulse voltammetry on the solutions of solids $2^{2\bullet}$, $3^{2\bullet}$, and $4^{2\bullet}$ in THF/TBAP give similar (except for current sign) current/potential curves compared to the carbodianions (Figure 4, Table III). These spectral data give further support for the structure and purity of the diradicals.

Solid diradicals are examined using a SQUID magnetometer. The products of magnetic susceptibility (χ) and temperature (T) are plotted versus temperature (T) at a constant applied magnetic

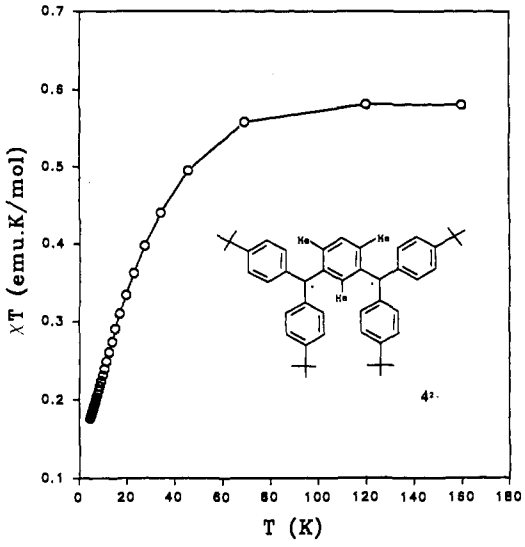

Figure 8. Plot of the product of magnetic susceptibility and temperature vs temperature for diradical $4^{2\bullet}$. SQUID data obtained at H = 5000 Oe.

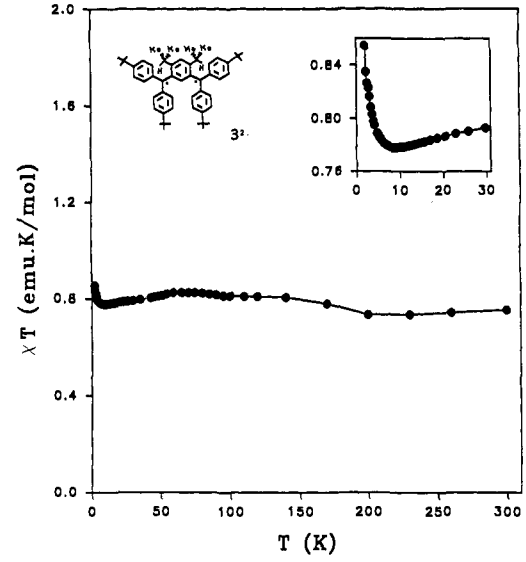

Figure 9. Plot of the product of magnetic susceptibility and temperature vs temperature for diradical $3^{2\bullet}$. SQUID data obtained at H = 500 Oe.

field (H) (Figures 7–9). Above T = 100 K, the χT product is approximately constant, and calculated effective magnetic moments, $\mu_{eff} = 2.823\ (\chi T)^{1/2}$, are 2.2 μ_B ($2^{2\bullet}$), 2.5 μ_B ($3^{2\bullet}$), and 2.2 μ_B ($4^{2\bullet}$). A calculated spin-only μ_{eff} for a paramagnet consisting of triplet molecules is 2.8 μ_B. Relatively lower μ_{eff} values for $2^{2\bullet}$ and $4^{2\bullet}$ compared to $3^{2\bullet}$ are in agreement with the results of the ESR spectra obtained after dissolving solid diradicals in 2-MeTHF (see preceding text).

For solid diradicals, both $2^{2\bullet}$ and $4^{2\bullet}$, the χT vs T plots turn downward at about T = 70 K (Figures 7 and 8). Furthermore, the normalized plots of magnetization (M/M_{sat}) vs H/T indicate spin, $S \leq {}^1/_2$, for both $2^{2\bullet}$ and $4^{2\bullet}$ at T = 2 and 5 K, respectively. Therefore, both $2^{2\bullet}$ and $4^{2\bullet}$ show antiferromagnetic interactions. The question is whether the interactions are intramolecular or intermolecular. In the case of the intermolecular interactions, the diradicals would be ground-state singlets and, in the other case, the diradicals would be ground-state triplets. For the singlet ground-state diradical with the thermally populated triplet excited state, magnetic susceptibility, χ, as a function of temperature should conform to the Bleaney–Bowers equation, and the triplet ESR signal should diminish at very low temperatures.[19] However,

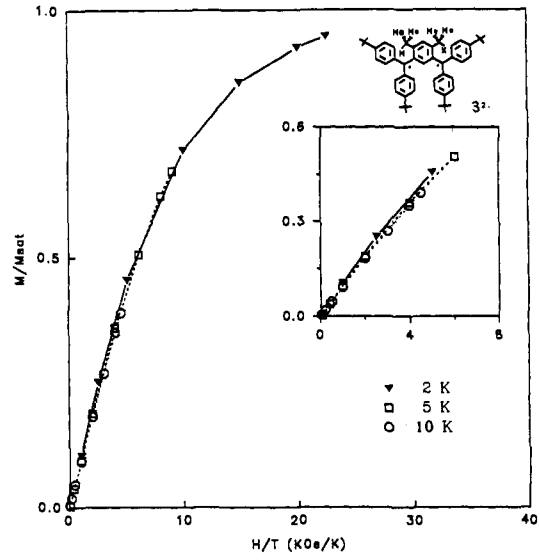

Figure 10. Normalized plots of magnetization vs the ratio of magnetic field and temperature for diradical $3^{2\bullet}$. SQUID data obtained at T = 2, 5, and 10 K.

the experimental χT vs T curves cannot be fit to the Bleaney–Bowers equation, and an intense ESR signal from a triplet state is observed for a dilute solution of diradical $2^{2\bullet}$ in 2-MeTHF glass at 4 K. Therefore, both $2^{2\bullet}$ and $4^{2\bullet}$ show the intermolecular antiferromagnetic interactions.

Interestingly, for solid diradical $3^{2\bullet}$, the χT vs T plot turns upward at about 4 K, suggesting an onset of short-range intermolecular ferromagnetic interactions between diradicals (Figure 9). This ferromagnetic behavior at low temperatures is confirmed by magnetization studies, that is, the normalized plots of magnetization (M/M_{sat}) versus H/T indicate slightly greater spin (S) at 2 K compared to 5 K and 10 K (Figure 10).[20] The M/M_{sat} vs H/T plots follow approximately a Brillouin function plot for S = 1; the sample is about 95% saturated at our lowest temperature and highest field (T = 2 K and H = 45 kOe). Ferromagnetic transition is not achieved at 2 K, however. No hysteresis of field-dependent magnetization could be detected at 2 K.

Conclusion

Methyl-substituted solid diradicals $2^{2\bullet}$ and $4^{2\bullet}$ show intermolecular antiferromagnetic interactions in the liquid nitrogen temperature range. Isopropyl-substituted solid diradical $3^{2\bullet}$ shows intermolecular ferromagnetic interactions in the liquid helium temperature range. Magnetic measurements at temperatures below 2 K would be needed to determine whether solid $3^{2\bullet}$ is a ferromagnet.

Although magnetic interactions in the solids made of diradicals $2^{2\bullet}$, $3^{2\bullet}$, and $4^{2\bullet}$ follow our tentative arguments based on steric hindrance, structural studies on solid diradicals are needed in order to further explore the correlation between structure and magnetism.

Experimental Section

Glovebox and Vacuum Lines. Air-sensitive dianions were handled using either glovebox or vacuum line techniques. UV–vis and electrochemistry studies were carried out in a glovebox (Vacuum Atmospheres Co.) that was equipped with a refrigerator, solvent trap, and vacuum line. Vacuum lines were similar to the line described previously.[21]

2-(OH)$_2$. *t*-BuLi (4.7 mL of 1.7 M solution in pentane, 8.0 mmol) was added to a solution of 4,6-dibromo-1,3-xylene (1.056 g, 4.000 mmol) in ether (40 mL) at −78 °C. After the solution was stirred for 1 h at −78 °C, 4,4′-di-*tert*-butylbenzophenone (1.178 g, 4.000 mmol) was added to the homogeneous reaction mixture. The temperature in the cooling bath was allowed to rise to 0 °C over a 1-h period, and then *t*-BuLi (4.7 mL,

(19) Bleaney, B.; Bowers, K. D. *Proc. R. Soc. London A* **1952**, 214. Kahn, O. *Angew. Chem., Int. Ed. Engl.* **1985**, *24*, 834. Krusic, P. J.; Wasserman, E. *J. Am. Chem. Soc.* **1991**, *113*, 2322.

(20) Extrapolation of M_{sat} for this sample was checked using another sample of $3^{2\bullet}$, for which the measurements were done at higher fields, i.e., T = 2 K and $H \leq$ 55 kOe.

(21) Rajca, A. *J. Org. Chem.* **1991**, *56*, 2557.

8.0 mmol) was added at −78 °C. After the solution was stirred for 2 h at −78 °C, 4,4′-di-*tert*-butylbenzophenone (1.178 g, 4.000 mmol) was added. The temperature was allowed to rise to 0 °C over a 2-h period, and then 10 mL of water was added. After extraction with ether and drying over $MgSO_4$, concentration in vacuo afforded 2.939 g of white glass. Crystallization from ethanol afforded colorless crystals, 1.905 g (68%): mp 266–267 °C; ^{1}H NMR ($CDCl_3$) 7.247 (d, J = 9, Hz, 8 H), 7.070 (d, J = 9 Hz, 8 H), 6.910 (s, 1 H), 6.810 (s, 1 H), 2.608 (s, 2 H), 2.046 (s, 6 H), 1.291 (s, 36 H); ^{13}C NMR ($CDCl_3$) δ 149.7, 143.4, 141.2, 136.2, 136.0, 130.4, 127.6, 124.5, 82.62, 34.38, 31.35, 21.53; ^{13}C DEPT (135°) (CH, CH_3) 136.2, 130.4, 127.6, 124.5, 31.35, 21.53. Anal. Calcd for $C_{50}H_{62}O_2$: 86.41; H, 8.99. Found: C, 86.25; H, 9.16.

2-(Cl)$_2$. Thionyl chloride (0.93 mL, 12.8 mmol) was added to a solution of **2-(OH)$_2$** (0.590 g, 0.850 mmol) in dry benzene (10 mL) and stirred for 1 h. Evaporation of the solvent afforded a yellow powder. Crystallization from hexane afforded 0.507 g (81%) of colorless crystals: ^{1}H NMR ($CDCl_3$) δ 7.452 (s, 1 H), 7.282 (d, J = 9 Hz, 8 H), 7.200 (d, J = 9 Hz, 8 H), 6.940 (s, 1 H), 1.873 (s, 6 H), 1.294 (s, 36 H).

2-(Br)$_2$. A solution of **2-(OH)$_2$** (95.8 mg, 0.138 mmol) in benzene (5 mL) was flushed with HBr gas for 30 min. Evacuation of the benzene afforded 96.7 mg (85% yield) of a light yellow solid: ^{1}H NMR ($CDCl_3$) δ 7.778 (s, 1 H), 7.246 (bs, 16 H), 6.915 (s, 1 H), 1.730 (s, 6 H), 1.294 (s, 36 H).

2-(OMe)$_2$. Trifluoroacetic anhydride (0.43 mL, 3.0 mmol) was added to a solution of **2-(OH)$_2$** (1.390 g, 2.000 mmol) in methylene chloride (50 mL) and stirred for 20 min, and then 100 mL of MeOH was added. After 1 h, 10% aqueous NaOH was added until pH > 7. After extraction with ether and drying over $MgSO_4$, concentration in vacuo afforded white glass (1.363 g). Treatment with boiling MeOH (150 mL), cooling to −20 °C, and filtration produced a white powder, 1.021 g (70%): mp 189–190 °C; FABMS (3-NBA), cluster m/z (peak height) at M^+ 722 (1), $(M - CH_2O)^+$ 692 (15), 693 (8), 694 (2.5); ^{1}H NMR ($CDCl_3$) δ 7.650 (s, 1 H), 7.265 (s, 16 H), 6.856 (s, 1 H), 2.947 (s, 6 H), 1.937 (s, 6 H), 1.283 (s, 36 H); ^{13}C NMR ($CDCl_3$) δ 149.14, 140.72, 137.92, 136.93, 136.57, 131.37, 128.21, 124.32, 87.72, 52.59, 34.33, 31.36, 21.39; ^{13}C DEPT (135°) (CH, CH_3) 136.57, 131.37, 128.21, 124.33, 52.59, 31.37, 21.40. Anal. Calcd for $C_{52}H_{66}O_2$: C, 86.37; H, 9.20. Found: C, 86.24; H, 9.14.

3-(OH)$_2$. *t*-BuLi (25.6 mL of 1.7 M solution in pentane, 43.5 mmol) was added to a solution of 4,6-dibromo-1,3-diisopropylbenzene (6.912 g, 21.73 mmol) in ether (200 mL) at −78 °C. After the solution was stirred for 1 h at −78 °C, 4,4′-di-*tert*-butylbenzophenone (6.34 g, 21.5 mmol) was added to the reaction mixture. The temperature in the cooling bath was allowed to rise to 0 °C over a 1-h period, and then *t*-BuLi (25.6 mL, 43.5 mmol) was added at −78 °C. After the mixture was stirred for 2 h at −78 °C, 4,4′-di-*tert*-butylbenzophenone (6.34 g, 21.5 mmol) was added. The temperature was allowed to rise to 0 °C over 2-h period, and then 10 mL of water was added. After extraction with ether and drying over $MgSO_4$, concentration in vacuo afforded light yellow glass (18.03 g). Crystallization from methanol afforded colorless crystals, 11.051 g (67%): mp 118.5–119.5 °C; ^{1}H NMR ($CDCl_3$) δ 7.272 (d, J = 9 Hz, 8 H), 7.257 (s, 1 H), 7.122 (d, J = 9 Hz, 8 H), 6.90 (s, 1 H), 3.109 (sep, J = 8 Hz, 2 H), 2.61 (s, 2 H), 1.292 (s, 36 H), 0.830 (d, J = 8 Hz, 12 H); ^{13}C NMR ($CDCl_3$) δ 149.62, 147.27, 143.96, 139.71, 128.50, 127.80, 126.56, 124.46, 82.40, 34.39, 31.35, 29.66, 23.83; ^{13}C DEPT (135°) (CH, CH_3) 128.51, 127.80, 126.57, 126.46, 31.36, 29.67, 23.83. Anal. Calcd for $C_{54}H_{70}O_2$: C, 86.35; H, 9.39. Calcd for $C_{54}H_{70}O_2(H_2O)$: C, 84.32; H, 9.44. Found: C, 84.43; H, 9.35.

3-(Br)$_2$. A solution of **3-(OH)$_2$** (0.396 g) in benzene (10 mL) was flushed with HBr gas for 30 min. Evacuation of the benzene afforded 0.4531 g (98%) of a light yellow solid: ^{1}H NMR ($CDCl_3$) δ 7.611 (s, 1 H), 7.363 (bs, 8 H), 7.315 (bs, 8 H), 7.262 (s, 1 H), 2.850 (sept, J = 8 Hz, 2 H), 1.294 (s, 36 H), 0.819 (d, J = 8 Hz, 12 H).

3-(OMe)$_2$. Trifluoroacetic anhydride (0.21 mL, 1.5 mmol) was added to a solution of **3-(OH)$_2$** (0.2255 g, 0.3001 mmol) in methylene chloride (15 mL) and stirred for 20 min, and then 50 mL of MeOH was added. After 1 h, 10% aqueous NaOH was added until pH > 7. After extraction with ether and drying over $MgSO_4$, concentration in vacuo afforded 0.2936 g of white glass. Crystallization from methanol afforded colorless crystals, 0.2149 g (92%): mp 216–217 °C; FABMS (3-NBA), cluster m/z (peak height) at M^+ 778 (1.5), 779 (1), $(M - CH_2O)^+$ 748 (14.5), 749 (8.5), 750 (2.5); ^{1}H NMR ($CDCl_3$) δ 7.750 (s, 1 H), 7.315 (d, J = 9 Hz, 8 H), 7.285 (d, J = 9 Hz, 8 H), 7.210 (s, 1 H), 2.945 (sep, J = 8 Hz, 2 H), 2.939 (s, 6 H), 1.282 (s, 36 H), 0.723 (d, J = 8 Hz, 12 H); ^{13}C NMR ($CDCl_3$) δ 149.14, 147.86, 141.35, 136.15, 129.18, 128.37, 126.94, 124.32, 87.58, 53.17, 34.34, 31.35, 29.26, 23.63; ^{13}C DEPT (135°) (CH, CH_3) 129.19, 127.38, 126.94, 124.32, 53.16, 31.35, 29.26, 23.64. Anal. Calcd for $C_{56}H_{74}O_2$: C, 86.32; H, 9.57. Found: C, 86.40; H, 9.56.

4-(OH)$_2$. *t*-BuLi (11.8 mL of 1.7 M solution in pentane, 20.0 mmol) was added to a solution of 2,4-dibromomesitylene (2.78 g, 10.0 mmol) in ether (100 mL) at −78 °C. After the solution was stirred for 1 h at −78 °C, 4,4′-di-*tert*-butylbenzophenone (2.94 g, 10.0 mmol) was added to the homogeneous reaction mixture. The temperature in the cooling bath was allowed to rise to 0 °C over a 1-h period, and then *t*-BuLi (11.8 mL, 20.0 mmol) was added at −78 °C. After this mixture was stirred for 2 h at −78 °C, 4,4′-di-*tert*-butylbenzophenone (2.94 g, 10.0 mmol) was added. The temperature was allowed to rise to 0 °C over a 2-h period, and then 15 mL of water was added. After extraction with ether and drying over $MgSO_4$, concentration in vacuo afforded 7.53 g of yellow glass. Crystallization from ethanol afforded a white powder (5.2 g). Recrystallization from hexane afforded colorless crystals, 4.98 g (70%): mp 256 °C dec; ^{1}H NMR ($CDCl_3$) δ 7.304 (d, J = 9 Hz, 8 H), 7.162 (d, J = 9 Hz, 8 H), 6.707 (s, 1 H), 2.712 (s, 2 H), 1.770 (s, 6 H), 1.506 (s, 3 H), 1.303 (s, 36 H); ^{13}C NMR ($CDCl_3$) δ 149.98, 144.53, 144.36, 139.92, 136.77, 133.94, 127.59, 124.87, 83.73, 34.43, 31.39, 25.64, 24.28; ^{13}C DEPT (135°) (CH, CH_3) 133.94, 127.59, 124.86, 31.39, 25.65, 24.28. Anal. Calcd for $C_{51}H_{64}O_2$: C, 86.39; H, 9.10. Found: C, 86.76; H, 9.93.

4-(OMe)$_2$. Trifluoroacetic anhydride (0.21 mL, 1.5 mmol) was added to a solution of **4-(OH)$_2$** (0.7091 g, 1.000 mmol) in methylene chloride (30 mL) and stirred for 20 min, and then 100 mL of MeOH was added. After 1 h, 10% aqueous NaOH was added until pH > 7. After extraction with ether and drying over $MgSO_4$, concentration in vacuo afforded 0.93 g of white glass. Treatment with boiling MeOH (200 mL), cooling to room temperature, and filtration produced a white powder, 0.63 g (60%): mp 228–229 °C; FABMS (3-NBA), cluster m/z (peak height) at M^+ 736 (3.5), 737 (2), $(M - CH_2O)^+$ 706 (14.5), 707 (7.5), 708 (2); ^{1}H NMR ($CDCl_3$) δ 7.240 (s, 16 H), 6.80 (s, 1 H), 3.193 (s, 6 H), 1.821 (s, 6 H), 1.349 (s, 3 H), 1.283 (s, 36 H); ^{13}C NMR ($CDCl_3$) δ 149.24, 143.07, 141.60, 139.91, 138.49, 134.90, 127.77, 124.34, 88.21, 51.54, 34.32, 31.40, 25.59, 24.51; ^{13}C DEPT (135°) (CH, CH_3) 134.89, 127.77, 124.33, 51.53, 31.40, 25.59, 24.50. Anal. Calcd for $C_{53}H_{68}O_2$: C, 86.36; H, 9.30. Calcd for $C_{53}H_{68}O_2$ (0.5 H_2O): C, 85.32; H, 9.32. Found: C, 85.59; H, 9.64.

Preparation of Carbodianions. Dianions were prepared by stirring of the ether precursor with lithium in THF. Vigorous stirring is essential for the purity of the dianions. For glovebox experiments (UV–vis and electrochemistry), THF was purified by distillation from Ph_2CO/Na and high-vacuum transfer from Ph_2CO/K (excess K). Lithium (Aldrich) of 98+% purity and high in sodium content was used.

NMR Spectroscopy. Samples for NMR studies were flame-sealed under vacuum in 5-mm NMR tubes. Chemical shifts are reported relative to TMS (0.00 ppm) using THF-d_8 (^{1}H; 3.580 ppm and ^{13}C, 67.45 ppm) as an internal standard. All spectra were obtained using a Bruker WM 400 spectrometer (400.1 MHz for ^{1}H, 100.6 MHz for ^{13}C). ^{13}C{^{1}H} NMR spectra of dianions at 303 K were obtained under the conditions allowing for integration of the quaternary carbons. Methanol was used as a standard for the low-temperature calibration.[22]

2^{2-},2Li$^+$: ^{1}H NMR (THF-d_8) δ *303 K* 6.997 (s, 1 H), 6.793 (s, 1 H), 6.743 (bs, 8 H), 6.516 (d, J = 9 Hz, 8 H), 1.935 (s, 6 H), 1.147 (s, 36 H), *283 K* 7.023 (s, 1 H), 6.775 (s, 1 H), 6.70 (bs), 6.502 (d, J = 9 Hz, 8 H), 1.934 (s, 6 H), 1.145 (s, 36 H), *263 K* 7.049 (s, 1 H), 6.756 (s, 1 H), 6.70 (coalescence), 6.485 (d, J = 9 Hz, 8 H), 1.930 (s, 6 H), 1.140 (s, 36 H), *243 K* 7.40 (bs, 4 H), 7.073 (s, 1 H), 6.743 (s, 1 H), 6.475 (d, J = 9 Hz, 8 H), 6.05 (bs, 4 H), 1.930 (s, 6 H), 1.414 (s, 36 H), *223 K* 7.45 (bs, 4 H), 7.091 (s, 1 H), 6.728 (s, 1 H), 6.462 (d, J = 9 Hz, 8 H), 6.000 (bs, 4 H), 1.927 (s, 6 H), 1.391 (s, 36 H); ^{13}C{^{1}H} NMR (THF-d_8) δ *303 K* 147.64 (2C), 145.59 (4C), 142.19, 133.72, 133.33 (2C), 128.46 (4C), 124.36, 118.51, 85.98, 33.94, 32.45, 21.49; ^{13}C DEPT (135°) (CH, CH_3) 142.19, 133.72, 124.35, 118.51, 32.44, 21.48, *283 K* 147.50, 145.46, 142.07, 133.60, 132.95, 128.16, 124.25, 118.4 (bs), 86.31, 33.88, 32.39, 21.56, *263 K* 147.41, 145.40, 141.93, 133.54, 132.62, 127.95, 124.2 (bs), 118.4 (coalescence), 86.74, 33.89, 32.41, 21.71, *243 K* 147.33, 145.33, 141.75, 133.48, 132.32, 127.77, 124.1 (bs), 121 (bs), 115 (bs), 87.10, 33.89, 32.41, 21.83, *223 K* 147.30, 145.32, 141.62, 133.46, 132.11, 127.66, 124.70, 123.82, 121.32, 115.32, 87.51, 33.94, 32.46, 21.99.

3^{2-},2Li$^+$: ^{1}H NMR (THF-d_8) δ *303 K* 7.170 (s, 1 H), 6.69 (s, bs, 9 H), 6.494 (d, J = 9 Hz, 8 H), 3.320 (sp, J = 8Hz, 2 H), 1.138 (s, 36 H), 1.037 (d, J = 8 Hz, 12 H); ^{13}C{^{1}H} NMR (THF-d_8) δ *303 K* 147.68 (2C), 146.53 (2C), 145.37 (4C), 143.74, 127.41 (4C), 124.11, 122.98, 117.80 (bs), 85.42, 33.84, 32.40, 29.70, 25.57; ^{13}C DEPT (135°) (CH, CH_2) 143.74, 124.11, 122.97, 32.40, 29.70, 25.57.

4^{2-},2Li$^+$: ^{1}H NMR (THF-d_8) δ *303 K* 6.783 (s, 1 H), 6.478 (d, J = 8 Hz, 8 H), 6.5 (bs, 8 H), 1.997 (s, 6 H), 1.921 (s, 3 H), 1.459 (s, 36 H); ^{13}C{^{1}H} NMR (THF-d_8) δ *303 K* 146.45 (2C), 144.49 (1C), 143.93 (4C), 135.01 (2C), 129.82, 125.94 (4C), 124.18, 116.83 (bs), 88.63,

(22) NMR temperature calibration: Raiford, D. S.; Fisk, C. L.; Becker, E. D. *Anal. Chem.* **1979**, *51*, 2050.

33.84, 32.50, 21.53, 17.87; ^{13}C DEPT (135°) (CH, CH_2) 129.83, 124.18, 32.50, 21.54, 17.88.

MeOH Quenching of Dianions Prepared from Diethers. A lithium piece (excess amount) was added to a solution of diether in THF (1 mL), allowed to stir for 24 h, and then quenched with MeOH. Extraction with ether afforded a white powder.

2-(H)$_2$. From 0.1427 g (0.1973 mmol) of **2**-(OMe)$_2$, 0.1283 g (98%) of product was obtained: mp 225–226 °C; ^1H NMR ($CDCl_3$) δ 7.182 (d, J = 8 Hz, 8 H), 6.910 (s, 1 H), 6.830 (d, J = 8 Hz, 8 H), 6.550 (s, 1 H), 5.475 (s, 2 H), 2.190 (s, 6 H), 1.280 (s, 36 H); ^{13}C NMR ($CDCl_3$) δ 148.45, 140.67, 140.07, 133.60, 132.10, 131.60, 128.85, 124.79, 51.98, 34.27, 31.38, 19.22; ^{13}C DEPT (135°) (CH, CH_3) 132.10, 131.60, 128.85, 124.79, 51.99, 31.39, 19.22. Anal. Calcd for $C_{50}H_{62}$: C, 90.57; H, 9.43. Calcd for $C_{50}H_{62}$(0.5 H_2O): C, 89.36; H, 9.45. Found: C, 89.51; H, 9.35.

3-(H)$_2$. 0.106 g (0.136 mmol) of **2**-(OMe)$_2$ was used to prepare 0.0882 g of product (90%): mp 214–215 °C; ^1H NMR ($CDCl_3$) δ 7.182 (d, J = 8 Hz, 8 H), 7.119 (s, 1 H), 6.814 (d, J = 8 Hz, 8 H), 6.487 (s, 1 H), 5.628 (s, 2 H), 3.230 (sept, J = 8 Hz, 2 H), 1.279 (s, 36 H), 1.128 (d, J = 8 Hz, 12 H); ^{13}C NMR ($CDCl_3$) δ 148.33, 143.88, 141.45, 138.02, 132.99, 128.92, 124.69, 121.55, 50.69, 34.27, 31.40, 28.52, 24.04; ^{13}C DEPT (135°) (CH, CH_3) 132.98, 128.92, 124.68, 121.56, 50.69, 31.39, 28.52, 24.04. Anal. Calcd for $C_{54}H_{70}$: C, 90.19; H, 9.81. Found: C, 90.15; H, 9.78.

4-(H)$_2$. Crude product (0.0832 g) was prepared from 0.1070 g (0.1450 mmol) of **4**-(OMe)$_2$. Treatment with boiling MeOH, cooling to room temperature, and filtration produced a white powder (0.0727 g). Preparative TLC (hexane/CH_2Cl_2 18:5) gave colorless crystals, 0.0653 g (90%): mp 214.0–214.5 °C; ^1H NMR ($CDCl_3$) δ 7.264 (s, J = 8 Hz, 8 H), 7.036 (d, J = 8 Hz, 8 H), 6.869 (s, 1 H), 5.959 (s, 2 H), 2.020 (s, 6 H), 1.729 (s, 3 H), 1.300 (s, 36 H); ^{13}C NMR ($CDCl_3$) δ 148.40, 139.59, 139.48, 137.70, 135.99, 132.05, 128.79, 124.81, 50.37, 34.32, 31.43, 21.96, 20.36; ^{13}C DEPT (135°) (CH, CH_3) 132.06, 128.79, 124.82, 50.37, 31.43, 21.97, 20.36. Anal. Calcd for $C_{51}H_{64}$: C, 90.47; H, 9.53. Calcd for $C_{51}H_{64}$(0.5 H_2O): C, 89.28; H, 9.55. Found: C, 89.52; H, 9.53.

Preparation of Diradicals 2$^{2\bullet}$, 3$^{2\bullet}$, and 4$^{2\bullet}$. A. From Dihalides 2-(Hal)$_2$ and 3-(Hal)$_2$. Deoxygenated and dry toluene (0.5 mL) was added to an evacuated tube containing dihalide (5 mg) and activated zinc powder (20 mg). (The zinc powder was treated with dilute hydrochloric acids, washed with distilled water, washed with acetone, and dried under vacuum.) After stirring for 20 min at 0 °C, the reaction mixture was examined using ESR spectroscopy.

B. From Diethers 2-(OMe)$_2$, 3-(OMe)$_2$, and 4-(OMe)$_2$. A lithium piece (excess amount) was added to a solution of diether (0.04 mmol) in THF (0.6 mL). The reaction mixture was stirred for 24 h in a glovebox. The solution of carbodianion was transferred to another vessel with a syringe. (An additional 0.2 mL of THF was used to complete the transfer.) Iodine (0.04 mmol) was added under a stream of argon to the solution of dianion at 0 °C on the vacuum line. After 15 min, 2-MeTHF or toluene (5 mL) was added using a Hamilton gas-tight syringe or vacuum transfer, and then an ESR spectrum was taken.

For the preparation of solid diradicals, solutions of dianions (0.1 mmol) in THF (1.3 mL) were used. Oxidations were done on the vacuum line in double-tube recrystallizers equipped with PTFE high-vacuum stopcocks and ultrafine glass frits (4–8 μm). After oxidation THF was removed under vacuum. The remaining solid residues were washed with deoxygenated MeOH. The green solids were dried under vacuum overnight (5×10^{-4} Torr) and then stored in the glovebox.

MeOH Quenching of Dianions Prepared from Diradicals. After ESR examination of a solution of diradical in 2-MeTHF/THF, excess lithium metal was added and the reaction mixture was stirred for 24 h. The disappearance of the ESR signal was followed. The red solution was quenched with MeOH. The usual workup afforded a white powder. ^1H NMR spectral data and melting points were consistent with the expected hydrocarbons, **2**-(H)$_2$, **3**-(H)$_2$, and **4**-(H)$_2$ (preceding data).

ESR Spectroscopy. A Bruker 200D SRC instrument was used to obtain the X-band ESR spectra. Temperatures in the range from 300 to 100 K were controlled by a nitrogen flow system equipped with a heat exchanger, Pt-resistance thermometer, and heater (Varian); temperatures were measured using a thermocouple. Temperatures in the 4 K range were controlled and measured using an Oxford Instruments ESR900 cryostat. Quartz ESR sample tubes (4-mm o.d.) connected to a high-vacuum stopcock (Kontes) via a graded seal were used for the spectra at 100 K; for spectra of reaction mixtures, the vessels possessed additional compartments. For spectra at 4 K, ESR tubes (with graded seals) were flame-sealed under vacuum.

Spectra of diradicals were obtained in dilute 2-MeTHF or toluene glasses. (For spectra of reaction mixtures, a small amount of THF was present.) All triplet diradicals had detectable Δm = 2 transitions.

UV-Vis Spectroscopy. UV-vis absorption spectra were recorded at ambient temperature in a 2-mm-pathlength quartz cell using a Perkin-Elmer Lambda 6 spectrophotometer. The spectrometer sample chamber was accessible from a glovebox. Preparations of all solutions were carried out in a glovebox under argon atmosphere.

Solutions of dianions were generated by adding an excess of Li metal into a stirring solution of the ether precursor in THF ($(1–2) \times 10^{-2}$ M). After the reaction was stirred for 24 h, the dianion solution was diluted with 2×10^{-4} M MeLi/THF to obtain a concentration that gave an appropriate absorbance.

Electrochemistry. All electrochemical measurements were carried out in a glovebox using a PARC Model 270 Electrochemistry System. THF was used as the solvent. The concentration of an electroactive solute was 0.001–0.003 M and of the supporting electrolyte, tetrabutylammonium perchlorate (TBAP), was 0.1–0.2 M. Three-electrode homemade voltammetric cells were used: a silver wire quasi-reference electrode, a Pt foil counter electrode, and a Pt disk working microelectrode (100-μm diameter, BAS). The solution volume was 2 mL. Typical CV scan rate was 200 mV/s. The differential pulse voltammetric parameters were as follows: scan rate = 20 mV/s; pulse amplitude = 25 mV; pulse width = 50 ms; pulse period = 0.2 s. Ferrocene (0.510 V vs SCE) was used as a reference.[23] The separation between potentials at the peaks of the oxidation and reduction CV waves was about 100 mV for ferrocene, dianions, and diradicals.

SQUID. Magnetic measurements were carried out using a SQUID magnetometer (MPMS, Quantum Design) at the University of Nebraska—Lincoln. The samples were prepared in the glovebox. The sample (20–30 mg) was packed in a bucket made from an ESR quartz tube (o.d. 5 mm, height 10 mm, 130–150 mg) and sealed with wax (30–50 mg). In order to prevent the sample from contacting hot wax, a piece of solid wax that fit the top part of the bucket was inserted before sealing with a layer of molten wax. The sample was then mounted in a straw that serves as a part of a sample holder. The sample was stored in an argon-filled tube during the transportation to the magnetometer site and before the measurement (4–48 h). Each data point was taken as the average of three scans after the sample had reached thermal equilibrium. Scan length and number of points per scan were 4 cm and 32 points, respectively. (The raw data, i.e., magnetic moment, "M", were positive below T = 200 K for diradicals.)

Background measurements were made on a bucket containing only wax. Molar susceptibilities at each temperature were obtained by dividing the corrected data by magnetic field and number of moles of diradical. Finally, susceptibilities of diradicals were corrected for core diamagnetism as calculated from Pascal's constants.[6]

Acknowledgment. We gratefully acknowledge the National Science Foundation for the support of this research (CHEM-8912762). We thank Professor Sy-Hwang Liou at the University of Nebraska for access to a SQUID magnetometer and discussions. We thank Dr. Anton Nazareth for helpful instruction in the operation of a SQUID magnetometer. FAB mass spectra were obtained at the Midwest Center for Mass Spectroscopy, a National Science Fundation Regional Instrumentation Facility (Grant No. CHE 8620177). We thank Mr. Alfred Weyerts for the design and construction of electrochemical cells.

Registry No. 2-(H)$_2$, 136575-85-4; **2-(OH)$_2$**, 136575-86-5; **2-(Cl)$_2$**, 136575-87-6; **2-(Br)$_2$**, 136575-88-7; **2-(OMe)$_2$**, 136575-89-8; **2$^{2\bullet}$**, 136575-90-1; **2^{2-},2Li$^+$**, 136576-00-6; **3-(H)$_2$**, 136575-91-2; **3-(OH)$_2$**, 136575-92-3; **3-(Br)$_2$**, 136575-93-4; **3-(OMe)$_2$**, 136575-94-5; **3$^{2\bullet}$**, 136575-95-6; **3^{2-},2Li$^+$**, 136576-01-7; **4-(H)$_2$**, 136575-96-7; **4-(OH)$_2$**, 136575-97-8; **4-(OMe)$_2$**, 136575-98-9; **4$^{2\bullet}$**, 136575-99-0; **4^{2-},2Li$^+$**, 136576-02-8; I_2, 7553-56-2; 4,6-dibromo-1,3-xylene, 615-87-2; 4,6-dibromo-1,3-diisopropylbenzene, 40734-61-0; 2,4-dibromomesitylene, 6942-99-0; 4,4′-di-*tert*-butylbenzophenone, 15796-82-4.

(23) Ferrocene: Diggle, J. W.; Parker, A. J. *J. Electrochem. Acta* **1973**, *18*, 976.